

A 40 GHz Air-Dielectric Cavity Oscillator with Low Phase Modulation Noise

Archita Hati, Craig W. Nelson, Bill Riddle, and David A. Howe

Abstract: We describe a 40 GHz cavity stabilized oscillator (CSO) that uses an air-dielectric cavity resonator as a frequency discriminator to reduce the phase modulation (PM) noise of a commercial 10 GHz dielectric resonator oscillator (DRO) frequency multiplied by four. Low PM noise and small size were the main design goals. Single sideband (SSB) PM noise equal to -128 dBc/Hz at a 10 kHz offset from the carrier frequency is achieved for the CSO. In addition, we report on the PM noise of several Ka-band components.

1. Introduction

Phase noise metrology is essential for the development and characterization of low noise, spectrally-pure oscillators. This paper focuses on the need for reference oscillators and measurements in the Ka-band (26.5 to 40 GHz), a large portion of which is authorized for U.S. military use. This requirement extends to millimeter wave data-communications and multistatic radar systems that place very stringent phase-stability requirements on system oscillators and components. Designing oscillators that operate at these high frequencies is challenging due to the frequency limitations of active devices.

One approach for generating a millimeter-wave reference signal is to simply multiply the frequency of a high quality factor (Q) quartz oscillator that is designed to operate at a lower sub-multiple frequency. However, multiplication techniques have their drawbacks. For example, the best low frequency oscillators are often bulky, costly and vibration sensitive. Also, frequency multipliers can increase PM noise at offset frequencies far from the carrier. When the signal from a low-noise oscillator is multiplied, its noise increases by $\log_{10}(N^2)$, where N is the multiplication factor. The noise of the frequency-multiplied signal is usually higher than the multiplier noise at offset frequencies close to the carrier, but lower at offset frequencies far from the carrier. Therefore, due to the inherent noise of the multiplier,

the low PM noise of an oscillator cannot be retained at higher frequencies by upconverting through frequency multiplication.

Some low noise microwave oscillators employ frequency locking to a high-Q resonance cavity to improve the broadband PM noise [1-5]. In these oscillators, the cavity resonator is used primarily as a frequency discriminator to improve the PM noise of the oscillator with a feedback control system. Any improvement of the discriminator phase-shift sensitivity directly translates to lowering the oscillator PM noise. There are several key aspects of controlling the cavity discriminator sensitivity, and the most important of these involves increasing the cavity Q [2, 6]. An effective method of increasing discriminator sensitivity is to suppress both the carrier signal reflected from the cavity, and the amplification of the residual noise [2, 3]. The suppression reduces the effective noise temperature of the nonlinear mixer, which acts as a phase detector with enhanced sensitivity. The amount of carrier suppression can be increased by making the effective coupling coefficient into the cavity approach its critical value of unity [2], and also by use of interferometric signal processing [4, 5]. The discriminator sensitivity is proportional to the power of the oscillator signal incident into the cavity [7]. Thus, by increasing the power of the carrier signal, the discriminator sensitivity can be improved as long as the resonator remains

linear, meaning that the power level does not change frequency. The purpose of this paper is to study the performance of an oscillator based on an air-dielectric cavity resonator that can be used as a measurement reference. These design considerations not only work in the development of a cavity-stabilized oscillator (CSO) of high spectral purity at 40 GHz, but have notable advantages when compared to the usual 10 GHz case.

Support for this work was provided by the Army Research Laboratory (ARL). For the purpose of technical description, commercial products are mentioned in this paper, but no endorsement by NIST is intended or implied.

Authors

Archita Hati¹
archita.hati@nist.gov

Craig W. Nelson²
craig.nelson@nist.gov

Bill Riddle³
bill.riddle@nist.gov

David A. Howe⁴
david.howe@nist.gov

^{1,2,4} Time and Frequency Division

³ Electromagnetics Division
National Institute of Standards
and Technology
325 Broadway
Boulder, Colorado, 80305

In Section 2 of this paper, we first provide the phase-noise performance of an assortment of active components at 40 GHz, including data that most manufacturers omit from their specifications. In Section 3, we discuss the design of our compact dielectric-cavity resonator. The CSO and its PM noise performance are described in Sections 4 and 5, respectively. Section 6 presents a summary.

2. PM Noise of Active Components at 40 GHz

The PM noise of individual components must be understood before they are included in a larger system, because the system performance is affected if a noisy component is selected. This section provides PM noise results for a few selective commercial components at Ka-band, since little or no information is available from the manufacturers.

We measured the noise of several amplifiers, dividers, and multipliers prior to the design of our 40 GHz oscillator to be discussed in Section 3. Figure 1 provides images of the components.

A single channel PM noise measurement system (Fig. 2) is used to measure noise of a pair of devices under test (DUTs) [8]. It uses a reference oscillator, a double balanced mixer (DBM), and a phase shifter. The oscillator signal is split into two to drive the input of each DUT. The outputs of the DUTs are connected to the LO and RF ports of a DBM that acts as a phase detector (PD). A phase shifter is used to establish phase-quadrature (90°) between two signals at the PD inputs required for phase noise measurement. The PD output produces voltage fluctuations at the baseband that are proportional to the difference between the phase fluctuations of DUT-1 and DUT-2. If the path lengths from the reference oscillator to the LO and RF ports are matched, the oscillator noise that is common mode cancels, to a large degree. The output of the PD after amplification is analyzed with a fast-Fourier-transform (FFT) spectrum analyzer. The voltage output of the IF amplifier is given by

$$v_n(t) = k_d G \Delta\phi(t), \quad (1)$$

where k_d is the PD's phase-to-voltage conversion factor, G is the gain of the IF amplifier and $\Delta\phi(t)$ is the difference between the phase fluctuations of the DUT-1 and DUT-2. Taking the Fourier transform of Eq. (1) provides

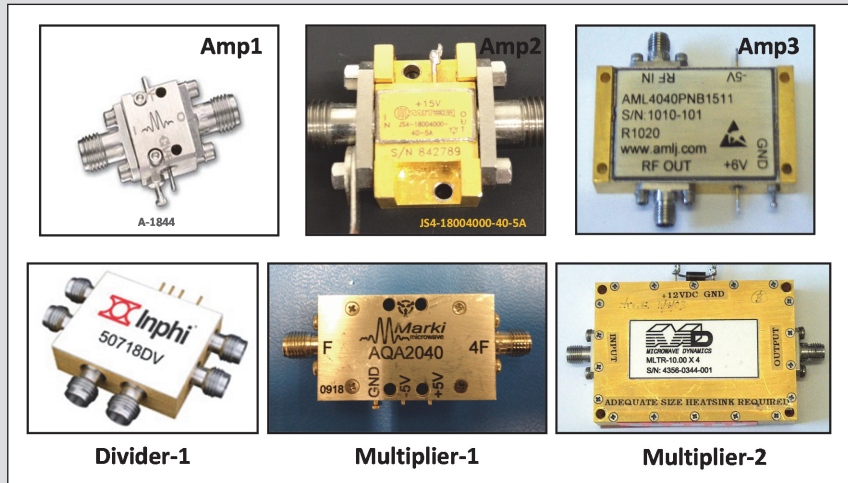


Figure 1. Images of commercial products used for PM noise measurement at 40 GHz.

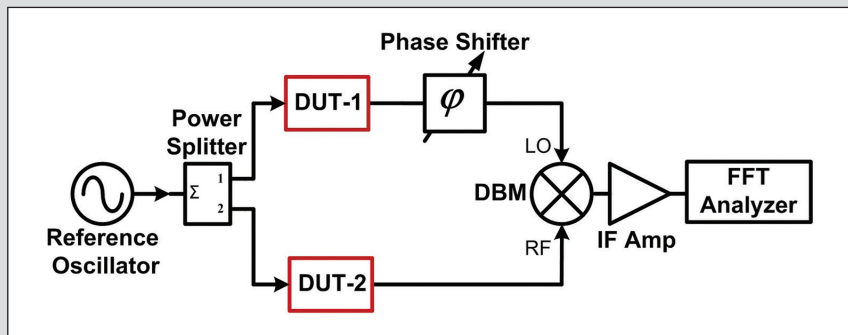


Figure 2. Block diagram of a single-channel system for measuring the PM noise of a pair of devices under test (DUTs).

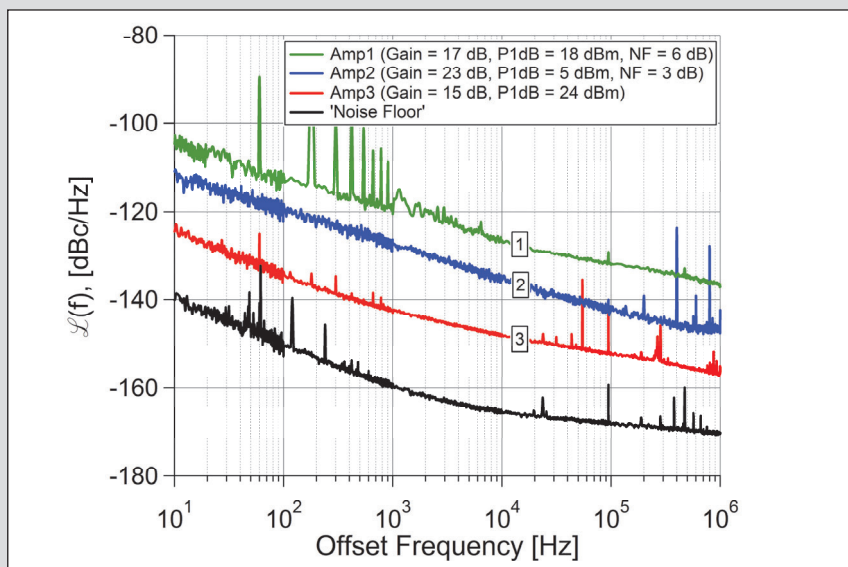


Figure 3. PM noise for a sample of commercial amplifiers (carrier frequency = 40 GHz).

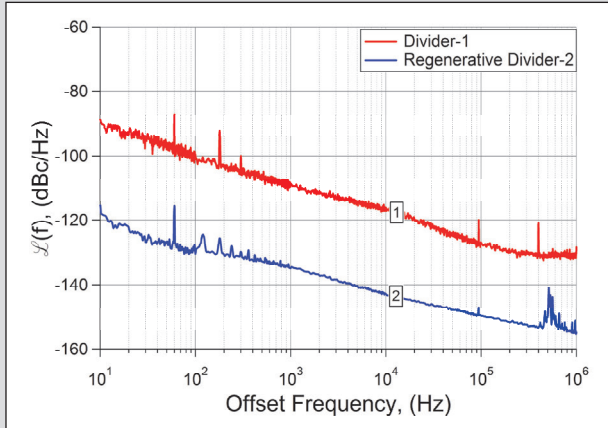


Figure 4. Input-referenced (i.e. 40 GHz) PM noise for a pair of dividers. Divider-1 is a commercial divider shown in Fig. 1. The regenerative divider is custom-built with two divide-by-2 in series. The input frequency is 40 GHz and the output frequency is 10 GHz.

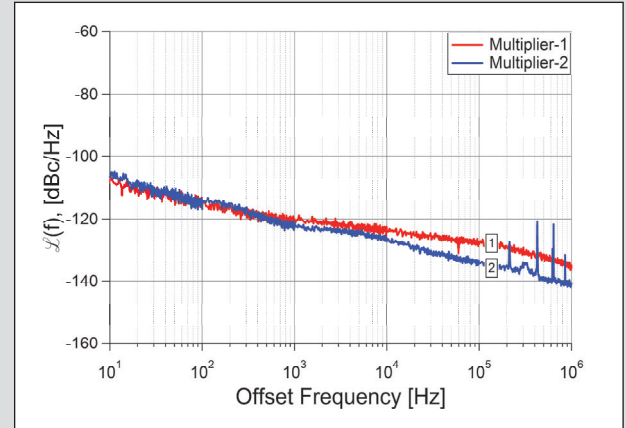


Figure 5. Output-referenced PM noise for a pair of multipliers. Multiplier-1 and Multiplier-2 are shown in Fig. 1. The input frequency is 10 GHz and the output frequency is 40 GHz.

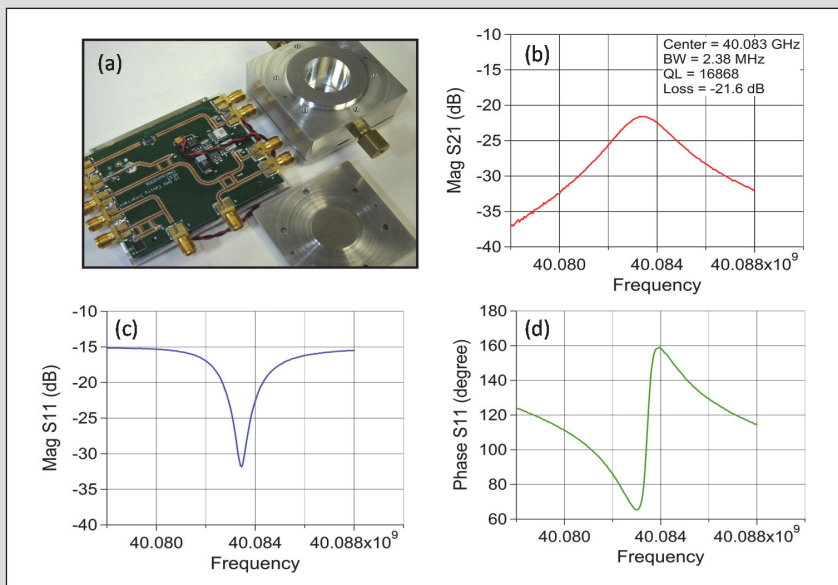


Figure 6. (a) Air-dielectric cylindrical aluminum cavity resonator at 40 GHz. The diameter ($2a$) and the length (d) of the cavity are approximately 2 cm. The SMA connectors on the circuit board can be used as a size reference. (b) Measured data of $|S_{21}|$ of a 40 GHz cavity. (c) Measured data of $|S_{11}|$ of a 40 GHz cavity. (d) Measured phase of S_{11} for a 40 GHz cavity.

$$S_{\varphi}(f) = \frac{PSD[v_n(t)]}{(k_d G)^2} = S_{\varphi,DUT}(f) + S_{\varphi,NF}(f) + \varepsilon^2 S_{\alpha}(f), \quad (2)$$

where $S_{\varphi}(f)$ is the measured PM noise, $S_{\varphi,DUT}(f)$ is the actual PM noise of a pair of DUTs, $S_{\varphi,NF}(f)$ is the measurement system noise floor comprised of PD and IF amplifier noise, $S_{\alpha}(f)$ is the measured amplitude modulation (AM) noise, ε is the AM-to-PM

conversion ratio, and PSD is the power spectral density. This measurement method is accurate as long as the PM noise of the DUT pairs is at least 10 dB higher than the PM noise floor of the measurement system and leakage AM noise. The noise floor of the measurement system is obtained simply by replacing the DUTs with coaxial cables or waveguide. However, it is important to keep the power level at the LO and RF ports at the same level for both the noise floor and the DUT measurements.

The calibration factor is obtained by measuring the voltage change (Δv) for a known static phase shift ($\Delta\Phi$). The fixed phase shift is first measured with a calibrated vector network analyzer (VNA). Thus, k_d can be obtained from the following equation,

$$k_d = \frac{\Delta v}{\Delta\Phi} \quad \frac{\text{volts}}{\text{radian}} \quad (3)$$

In the case of amplifiers, only one DUT can be used if an equal amount of delay is introduced to substitute for DUT-2. This prevents incomplete cancellation of the reference oscillator noise at higher offset frequencies.

Figure 3 shows the single-sideband PM noise, $\mathcal{L}(f) \left(\equiv \frac{1}{2} S_{\varphi}(f) \right)$ of three commercially available amplifiers. Note that Amp1 and Amp3 have approximately the same gain and P1 dB compression, but that there is a variation of almost 20 dB in the PM noise performance. A similar variation in noise occurs for the two dividers shown in Fig. 4. We compared the noise of two dividers: one commercial (pictured in Fig. 1) and the other a custom regenerative divide-by-four (two divide-by-two in series) [9, 10]. In addition, we compared the noise of two frequency multipliers (Fig. 5). The large differences in noise performance between the various devices indicate the importance of selecting the correct components when designing a low-noise system for this frequency band.

The 2-sigma combined fractional uncertainties of the PM noise measurement system discussed above is approximately

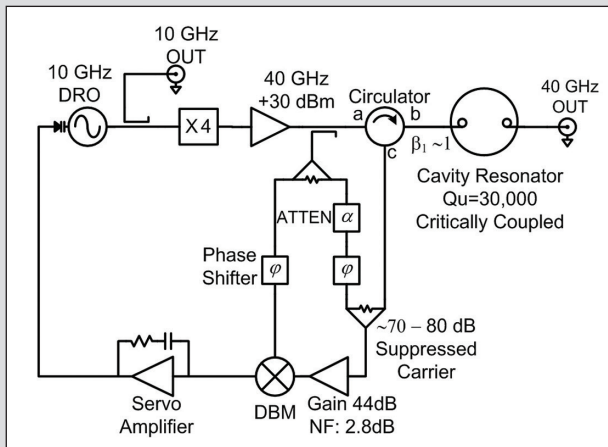


Figure 7. Block diagram of the cavity stabilized oscillator (CSO) at 40 GHz.

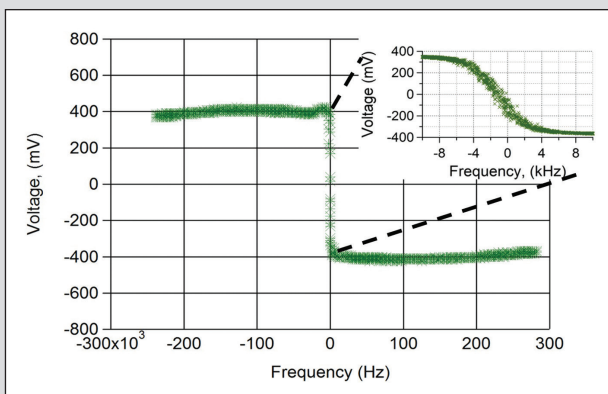


Figure 8. Typical error signal from the double-balanced mixer (DBM) in the cavity discriminator of Fig. 7. The inset corresponds to a slope of 100 mV/kHz, approximately, for the resonator discriminator curve.

1.4 dB, which is obtained by combining the individual uncertainties, evaluated with both Type A and Type B methods [11, 12]. The contribution to uncertainty from a Type A evaluation is 1.2 dB, due to the number of FFT averages used for PM and AM noise measurements and measurement repeatability. The contributors to uncertainty evaluated with the Type B method include the calibration of k_d , the measurement of IF amplifier gain and its frequency response, AM-to-PM conversion at the PD, and error in the estimated measurement bandwidth of the PSD function. The contribution to uncertainty from components evaluated with the Type B method is conservatively estimated as approximately 0.7 dB.

3. Compact Air-Dielectric Cavity Resonator

An important goal of microwave oscillator design is to achieve significant reductions in size, weight, and power (so-called SWaP) without a noise penalty. This paper investigates one strategy of reducing SWaP while maintaining state-of-the-art spectral purity. The basic approach used in the past at the National Institute of Standards and Technology (NIST) consisted of improving the PM noise of a 10 GHz voltage-controlled oscillator (DRO, yttrium iron garnet (YIG)

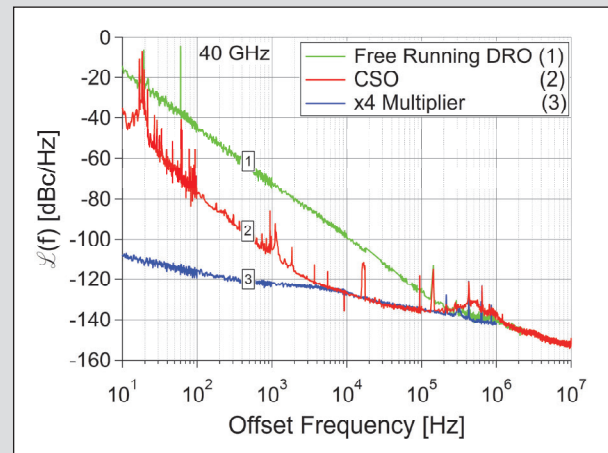


Figure 9. PM noise of a cavity stabilized oscillator (CSO), the results are normalized to 40 GHz. Notice the significant noise reduction of the free-running DRO noise out to beyond the 100 kHz offset frequency.

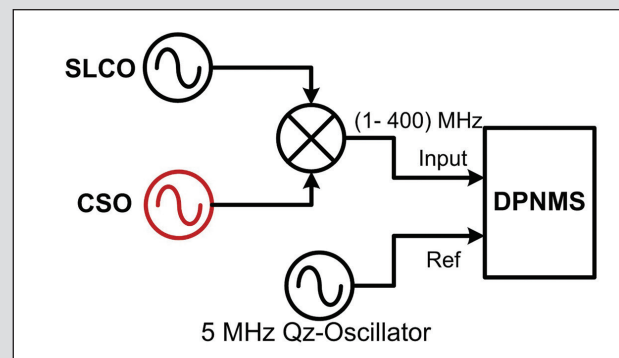


Figure 10. Experimental set-up of CSO PM noise measurement (SLCO = sapphire loaded cavity oscillator, DPNMS = digital phase noise measurement system).

oscillator, etc.) by use of a high-Q, highly linear air-dielectric 10 GHz cavity as a discriminator [7]. The unloaded Q's (Q_u) of 50,000 to 70,000 are attained for TE023 or TE025 modes, but achieving this moderately high Q_u resulted in a fairly large cavity diameter and a height of approximately 8 cm. With only a minimal increase in noise, we can substitute a significantly smaller 40 GHz highly-linear air-dielectric cavity as a discriminator. The air-dielectric cylindrical cavity used in the CSO design is operating at TE015 mode, and its inside dimensions are approximately 2 cm \times 2 cm (about one-fourth the size of NIST's 10 GHz cavity resonator). The resonant frequency of this cylindrical cavity is given by [13]

$$f_{res} = \frac{c}{2\pi} \sqrt{\left(\frac{3.832}{a}\right)^2 + \left(\frac{5\pi}{d}\right)^2}, \quad (4)$$

where a and d are the radius and length of the cylindrical cavity, respectively. For $2a \approx d \approx 2$ cm, the resonant frequency is approximately 40.08 GHz.

The cavity is made of aluminum (Al), and the inside surface of the cylinder and end caps are electro-silver plated and polished to

Offset frequency (Hz)	CSO	Micro-optoelectronic oscillator [22]	Phase locked dielectric resonator oscillator [23]	Voltage controlled oscillator [24]	Commercial frequency synthesizer [25]
100	-78	-54	-61	+8	-83
1000	-105	-84	-96	-28	-105
10000	-128	-107	-103	-71	-117
100000	-135	-119	-106	-96	-115

Table 1. PM noise comparison of different Ka-band oscillators at 40 GHz.

an industry standard of less than 0.2 μm root mean squared, considered to be a mirror finish, with a plate thickness of 50 μm .

The cavity used for the CSO design is shown in Fig. 6(a). The signal is coupled to the magnetic field in and out of the cavity by use of coupling probes (loops) on the end plates with their planes aligned with the radial plane of the cylindrical cavity. A VNA is used to measure both Q_u and the loaded quality factor, Q_L , and also to characterize the S-parameters of the resonator. For the measurement of Q_u both the input and output coupling probes are loosely coupled, whereas for Q_L the coupling probes are adjusted to obtain nearly critical input and loose output couplings. The Q_u and Q_L are calculated from the ratio of the resonant frequency to the 3 dB bandwidth. The measured values of these quantities for the 40 GHz resonator are approximately 30,000 and 17,000.

The typical formulas for the reflection (S_{11}) and transmission (S_{21}) coefficients in terms of input (β_1) and output (β_2) coupling coefficients at the cavity resonance frequency are [7, 14, 15],

$$S_{11} = \frac{1 - \beta_1 + \beta_2}{1 + \beta_1 + \beta_2}, \quad S_{21} = \frac{2\sqrt{\beta_1\beta_2}}{1 + \beta_1 + \beta_2}. \quad (5)$$

For β_1 and β_2 equal to 0.94 and 0.01, the reflected and the transmitted signals out of the cavity are suppressed by approximately 32 dB and 22 dB, respectively, as shown in Fig. 6. The nearly critical coupling coefficient (0.94) is chosen because it provides a steeper discriminator curve (higher discriminator sensitivity). Any improvement to the discriminator phase-shift sensitivity directly translates to a reduction of oscillator PM noise. An effective method of increasing discriminator sensitivity is to suppress the carrier signal reflected from the cavity, which can be achieved by making the effective coupling coefficient into the cavity approach

its critical value of unity. An output coupling of 0.01 was chosen because with high incident power of almost 1 W to the cavity, it is possible to obtain reasonable output power (nearly 10 dBm) for the final stabilized oscillator directly from the transmission port of the cavity without further degrading the cavity Q.

4. Description of the CSO

Figure 7 is a block diagram of the CSO at 40 GHz. It consists of a DRO (dielectric resonator oscillator) at 10 GHz whose free-running PM noise is approximately -112 dBc/Hz at a 10 kHz offset frequency. The output of the DRO is first multiplied by four and then amplified to 1 W, by use of a power amplifier. The amplified signal is then applied to the input coupling port of the discriminator cavity through a circulator. The reflected signal out of the cavity exits port 'c' of the circulator and is already highly suppressed because the cavity coupling is nearly critical. A portion of the input signal is added out of phase with the reflected signal to further suppress the carrier (to about -50 dBm). This constitutes the so-called interferometric signal processing. The suppressed-carrier signal is then amplified by use of a low-noise amplifier (gain = 44 dB, noise figure = 2.8 dB) before being applied to one port of a DBM that acts as a phase detector. Due to the high level of carrier suppression, the amplifier's flicker noise contribution is significantly reduced. The other port of the DBM is a directionally-coupled portion of the input signal, adjusted to be in phase quadrature with the reflected signal. By placing the amplifier before the mixer, the effective noise contribution from the mixer is suppressed by the amplifier gain. The output of the DBM is the error voltage that tracks the frequency fluctuations of the DRO relative to the cavity. This error voltage is applied to the voltage-control tuning input of the DRO through the servo amplifier to stabilize its frequency.

Figure 8 shows a typical error signal at the output of the DBM versus the frequency difference between the resonance frequency of the cavity and the 10 GHz DRO signal multiplied by four. This slope, which is at the mid-point of the resonator discriminator curve, is approximately 100 mV/kHz.

The dimension of the prototype CSO is approximately 30 cm \times 30 cm \times 10 cm, and we expect to further reduce the size in our final design by replacing the connectorized components with a microstrip layout. The 10 GHz reference oscillator weighs over 15 kg and is assembled inside a 6U chassis with 43 cm depth in a standard rack mount.

5. PM Noise Results

Figure 9 shows the PM noise of a 40 GHz CSO constructed with an aluminum air-dielectric cavity designed for the candidate mode TE₀₁₅ with an unloaded Q of about 30,000. The noise is measured at 10 GHz at the input of the $\times 4$ multiplier due to the unavailability of a 40 GHz reference oscillator, which has either comparable or lower PM noise than the CSO.

The PM noise measurement scheme (Fig. 10) utilizes a direct-digital phase noise measurement system (DPNMS) [16, 17]. The DPNMS (1) directly measures relative phase and does not require a phase-locked reference at the same frequency, and (2) contains a dual-channel, cross-correlation technique to reduce DPNMS-system random noise and low-level digitally generated artifacts, or spurs. A DPNMS requires a reference oscillator with noise below the test oscillator. The operating frequency range of this DPNMS used is 1 MHz to 400 MHz. In order to measure the PM noise of the CSO at 10 GHz, this signal is mixed with a 10.001 GHz signal from a sapphire loaded cavity oscillator (SLCO) to down-convert the 10 GHz signal to within the operational frequency range of the DPNMS. The down-converted signal is then compared against a low PM noise signal obtained from a 5 MHz quartz crystal oscillator. The noise floor of the measurement system is determined by replacing the CSO with a second SLCO. The noise floor ranges from 15 to 20 dB lower than the PM noise of the CSO at a 10 GHz output.

The final results shown in Fig. 9 are normalized to 40 GHz. The PM noise of the free-running DRO is shown along with the CSO that demonstrates a 30 to 35 dB reduction in the PM noise of the free-running DRO. The origin of random-walk noise (f^{-4})

and spurious close-to-the carrier noise is due to the temperature and vibration sensitivities of the resonator. The source of flicker frequency noise (f^{-3}) between 100 Hz to 2 kHz is due to flicker phase noise (f^{-1}) originating inside the discriminator, likely from the circulator, DBM, and carrier suppression amplifier [7], and also possibly from AM-to-PM conversion in the DBM. Above 2 kHz the noise of the CSO is consistent with and clearly limited by the $\times 4$ multiplier noise, or the bottom-most noise. The broad structure around 500 kHz offset is due to the discriminator servo loop.

Note that the multiplier PM noise shown in Fig. 9 is measured with analog measurement system already discussed in Section 2 (Fig. 5). The DPNMS is used to measure noise at offset frequencies from 10 Hz to 100 kHz. Above a 100 kHz offset, a photonic delay-line measurement system (PDLMS) [18, 19] is utilized because it has less instrument noise above 100 kHz than the DPNMS. It is common practice to use such hybrid schemes to cover a large range of offsets frequencies. Providing a complete accounting of the measurement uncertainties is beyond the scope of this paper, but we can summarize by stating that the measurement uncertainty of the DPNMS is less than 1 dB and the measurement uncertainty of the PDLMS is less than 2 dB. Both systems were calibrated against NIST's PM/AM secondary noise standard [20, 21].

There are two drawbacks of measuring the PM noise at the input of the multiplier at 10 GHz. First, the measured noise at 10 GHz is limited by the $\times 4$ multiplier noise. Any corrections to the 40 GHz signal that are lower than the multiplier noise cannot be detected at the 10 GHz output. Second, any improvements to the 40 GHz signal at frequencies far from the carrier due to the passive filtration of the cavity cannot be observed. There are strategies that can be used to reduce the $\times 4$ multiplier noise, hence reduce the DRO noise, given that the multiplier's output is phase stabilized by the overall CSO scheme. The simplest strategy would be to simply replace the "DRO $\times 4$ " with a single low-noise 40 GHz voltage-controlled oscillator (VCO). However, candidates for a sufficiently low-noise phase-lockable oscillator are not commonly available at a 40 GHz center frequency. Table 1 shows the performance of the CSO with respect to few commercially available oscillators in the Ka-band. The PM noise of all oscillators is normalized to 40 GHz. This comparison is done only in terms of PM noise; their size, cost and power consumption are not taken into consideration.

6. Conclusions

We measured the PM noise of several commercially available Ka-band components and observed wide variations in the noise performance among devices. These results indicate how important it is to correctly select components when designing a low-noise oscillator in the Ka frequency band. We also reported performance of a low-PM noise 40 GHz CSO using an air-dielectric cavity resonator as a frequency discriminator. The cavity in TE015 mode has an unloaded Q of 30,000. The PM noise of the CSO at 10 kHz offset is -128 dBc/Hz and is entirely limited by the multiplier noise. In the future we plan

- to use a 40 GHz VCO instead of a 10 GHz DRO and a $\times 4$ multiplier,
- to control the cavity temperature and use vibration isolation to reduce close-to-the carrier noise, and
- to use an ultra-stiff ceramic cavity resonator to improve the vibration sensitivity of the oscillator.

7. Acknowledgements

The authors thank Justin Lanfranchi for the construction and noise measurement of 40 GHz regenerative divide-by-four circuit, and Stefania Römisch and Jeff Jargon for useful discussion and suggestions. We also thank Danielle Lirette and David Smith for carefully reading and providing comments on this manuscript.

8. References

- [1] F. Walls, C. Felton, and T. Martin, "High Spectral Purity X-Band Source," *Proceedings of 1990 IEEE International Frequency Control Symposium*, Baltimore, Maryland, pp. 542-548, May 1990.
- [2] D. Santiago and G. Dick, "Microwave Frequency Discriminator with a Cooled Sapphire Resonator for Ultra-Low Phase Noise," *Proceedings of 1992 IEEE International Frequency Control Symposium*, Hershey, Pennsylvania, pp. 176-182, May 1992.
- [3] D. Santiago and G. Dick, "Closed Loop Tests of the NASA Sapphire Phase Stabilizer," *Proceedings of 1993 IEEE International Frequency Control Symposium*, Salt Lake City, Utah, pp. 774-778, June 1993.
- [4] E. Ivanov, M. Tobar, and R. Woode, "Advanced Phase Noise Suppression Technique for Next Generation of Ultra Low-Noise Microwave Oscillators," *Proceedings of 1995 IEEE International Frequency Control Symposium*, San Francisco, California, pp. 314-320, May 1995.
- [5] E. Ivanov, M. Tobar, and R. Woode, "Applications of interferometric signal processing to phase-noise reduction in microwave oscillators," *IEEE T. Microw. Theory*, vol. 46, no. 10, pp. 1537-1545, October 1998.
- [6] M. Tobar, E. Ivanov, R. Woode, and J. Searls, "Low Noise Microwave Oscillators Based on High-Q Temperature Stabilized Sapphire Resonators," *Proceedings of 1994 IEEE International Frequency Control Symposium*, Boston, Massachusetts, pp. 433-440, June 1994.
- [7] A. Gupta, D. Howe, C. Nelson, A. Hati, F. Walls, and J. Nava, "High spectral purity microwave oscillator: design using conventional air-dielectric cavity," *IEEE T. Ultrason. Ferr.*, vol. 51, no. 10, pp. 1225-1231, 2004.
- [8] F. Walls and E. Ferre-Pikal, "Measurement of frequency, phase noise and amplitude noise," *Wiley Encyclopedia of Electrical and Electronics Engineering*, vol. 12, pp. 459-473, June 1999.
- [9] R. Miller, "Fractional-frequency generators utilizing regenerative modulation," *P. IRE*, vol. 27, no. 7, pp. 446-457, 1939.
- [10] E. Rubiola, M. Olivier, and J. Gros Lambert, "Phase noise in the regenerative frequency dividers," *IEEE T. Instrum. Meas.*, vol. 41, no. 3, pp. 353-360, June 1992.
- [11] JCGM, "Evaluation of measurement data — Guide to the expression of uncertainty in measurement," *JCGM 100*, 2008.
- [12] B. Taylor and C. Kuyatt, "Guidelines for Evaluating and Expressing the Uncertainty of NIST Measurement Results," *NIST Technical Note 1297*, 1994.
- [13] D. Pozar, *Microwave Engineering*, 3rd ed., John Wiley & Sons, 2009.
- [14] E. Ginzton, *Microwave Measurements*, McGraw-Hill Book Company Inc., 1957.
- [15] L. Chen, C. Ong, C. Neo, V. Varadan, and V. Varadan, *Microwave Electronics: Measurement and Materials Characterization*, John Wiley & Sons, 2004.

- [16] J. Grove, J. Hein, J. Retta, P. Schweiger, W. Solbrig, and S. Stein, "Direct-digital phase-noise measurement," *Proceedings of 2004 IEEE International Frequency Control Symposium*, Montreal, Canada, pp. 287-291, August 2004.
- [17] C. Nelson and D. Howe, "A Sub-Sampling Digital PM/AM Noise Measurement System," *NCSLI Measure J. Meas. Sci.*, vol. 7, no. 3, pp. 70-73, 2012.
- [18] E. Rubiola, E. Salik, S. Huang, N. Yu, and L. Maleki, "Photonic-delay technique for phase-noise measurement of microwave oscillators," *J. Opt. Soc. Am. B*, vol. 22, no. 5, pp. 987-997, 2005.
- [19] <http://www.oewaves.com/phase-noise-measurement>
- [20] F. Walls, "Secondary standard for PM and AM noise at 5, 10 and 100 MHz," *IEEE T. Instrum. Meas.*, vol. 42, no. 2, pp.136-143, 1993.
- [21] A. Hati, C. Nelson, N. Ashby, and D. Howe, "Calibration uncertainty for the NIST PM/AM noise standards," *NIST Special Publication 250-90*, 33 p., July 2012.
- [22] <http://www.oewaves.com/products/item/85-micro-opto-electronic-oscillator-oeo.html> (<http://www.fh-microwave.com/produits-products/photonics/>)
- [23] <https://miteq.com/docs/MITEQ-PLDRO40000.PDF>
- [24] <https://www.hittite.com/products/view.html/view/HMC-C073>
- [25] <http://cp.literature.agilent.com/litweb/pdf/5989-0698EN.pdf>